



## Bifacial PV cell with reflector for stand-alone mast for sensor powering purposes

**Jakobsen, Michael Linde; Thorsteinsson, Sune; Poulsen, Peter Behrendorff; Riedel, Nicholas; Rødder, Peter Melchior; Rødder, Kristin**

*Publication date:*  
2017

*Document Version*  
Publisher's PDF, also known as Version of record

[Link back to DTU Orbit](#)

*Citation (APA):*  
Jakobsen, M. L., Thorsteinsson, S., Poulsen, P. B., Riedel, N., Rødder, P. M., & Rødder, K. (2017). *Bifacial PV cell with reflector for stand-alone mast for sensor powering purposes*. Paper presented at 13th International Conference on Concentrator Photovoltaic Systems , Ottawa, Canada.

---

### General rights

Copyright and moral rights for the publications made accessible in the public portal are retained by the authors and/or other copyright owners and it is a condition of accessing publications that users recognise and abide by the legal requirements associated with these rights.

- Users may download and print one copy of any publication from the public portal for the purpose of private study or research.
- You may not further distribute the material or use it for any profit-making activity or commercial gain
- You may freely distribute the URL identifying the publication in the public portal

If you believe that this document breaches copyright please contact us providing details, and we will remove access to the work immediately and investigate your claim.

# Bifacial PV cell with reflector for stand-alone mast for sensor powering purposes

Michael L. Jakobsen<sup>1, c)</sup>, Sune Thorsteinsson<sup>1, b)</sup>, Peter B. Poulsen<sup>1, a)</sup>, N. Riedel<sup>1</sup>, Peter M. Rødder<sup>2</sup> and Kristin Rødder<sup>2</sup>

<sup>1</sup> *Department of Photonics Engineering, Technical University of Denmark, mlja@fotonik.dtu.dk, Roskilde, Denmark.*

<sup>2</sup> *SolarLab, pmr@solarlab.dk, Viby J., Denmark.*

<sup>a)</sup>Corresponding author: ppou@fotonik.dtu.dk

<sup>b)</sup>sunth@fotonik.dtu.dk

<sup>c)</sup>mlja@fotonik.dtu.dk

**Abstract.** Reflectors to bifacial PV-cells are simulated and prototyped in this work. The aim is to optimize the reflector to specific latitudes, and particularly northern latitudes. Specifically, by using minimum semiconductor the reflector must be able to deliver the electrical power required at minimum the condition of solar travel above the horizon, worst weather condition etc. We will test a bifacial PV-cell with a retroreflector, and compare the output with simulations combined with local solar data.

## INTRODUCTION

Bifacial solar modules are commercially attractive, due to the fact that the total energy producing area increases by a factor of two, and only to an additional module cost of approximately 30 %.<sup>1</sup> However, the challenge is to guide light onto both sides sufficiently efficient. Several works have proven that adding reflectors to bifacial panels mounted at a certain optimized tilt, increases the energy harvest even further,<sup>2-3</sup> and bifacial panels has offered new solutions as e.g. PV based fences.<sup>4</sup> For PV-systems mounted at a tilt, the reflectors will in many cases be placed underneath the PV panel to reflect incident light from surroundings e.g. the albedo. Since these reflectors are not exposed to rain they do not have the same self-cleaning ability as the PV panels itself and the resulting energy harvest is decreased due to soiling.<sup>2,4</sup>

Earlier, we have proposed a system, using a vertical mounted bifacial panel and two vertical reflectors<sup>5</sup> mounted at an angle to partly reduce the soiling problem, but also to optimize the energy harvest. The schematics is illustrated in figure 1. The investigation of this system has been based on raytracing with different assumptions to simplify the model. One of the assumptions is that the irradiance of sunlight incident onto a surface, being normal to the sun all day, is constant.

The conclusions on the following investigations were that the bifacial PV-cell, combined with a retroreflector, including a transparent filling material, could collect 96 % of all light, incident onto a plane surface with the same area as both sides of the bifacial PV-cell together.<sup>6</sup> With and without the filling the simulated amount of incident light is plotted in figure 2 as a function of azimuth angular position of the sun.

In this work, we will include experimental solar data to estimate a more realistic incidence of sunlight in our simulations to finalize our model, and to compare it with data from an experimental prototype (see figure 3). This will bring us to a discussion where we can compare this device with a bifacial PV-cell without a reflector and an ordinary plane PV-cell.

## THE MODEL

Two types of optical losses are modelled within this work:

- Fresnel losses, which are optical losses at the interfaces of the dielectric media covering the PV cell.
- Material absorption losses due to either propagation in bulk material or reflection at the metallic surface.

The Fresnel losses are determined by using the Fresnel equations for the TE and TM polarization modes at incidence onto the covering material.

Material absorption losses occurring due to absorption when light propagates inside a transparent dielectric material can be neglected here, because the covering material above the PV cells is where thin ( $< 1$  mm). However, the reflection coefficients for the metallic surfaces are significant, and here they are set to 95% for enhanced alumina.

Initially, a design according to Fig.1 is used for the raytracing model, and in the first design the mirrors are plane surfaces and thus provide no concentration of the sunlight. The system comprises of a vertical standing bifacial panel, which for simulation purposes is oriented east west, and two reflector plates extending in angles ( $\alpha = \pm 45$  deg.) relative to the bifacial panel. In this work, the reflector encapsulates only half the length of the PV cell, which in total is  $2 L_p$ .

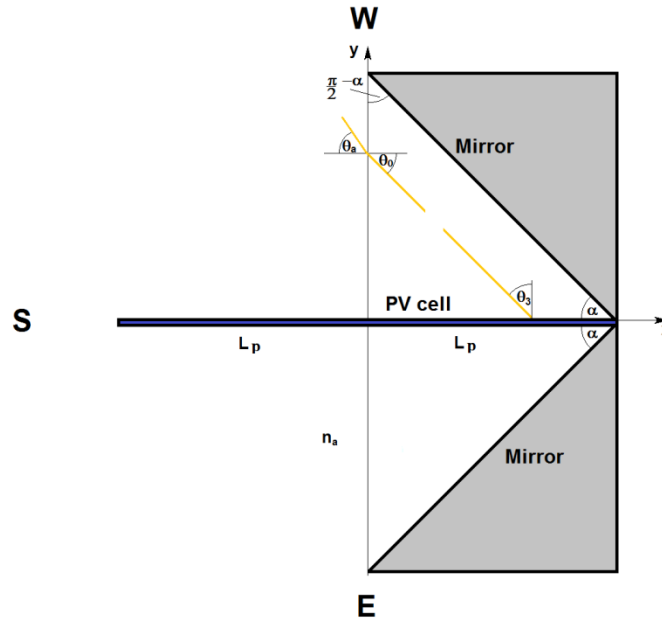


**FIGURE 1.** Illustration of the reflector system.

Ray tracing, where many optical rays are modelled and finally the weighted output is integrated, are performed on this system. Earlier designs had a bulk material inside the reflector, in order to capture light reflected by the reflector in an unfortunate direction, and thus leaving the retroreflector. The capture is achieved by internal total reflection. However, in this case the volume inside the reflector consists of air. The extension of the PV cell the length of  $L_p$  away from the retroreflector means that all these escaping light rays are captured directly by the PV cell.

We assume that all light incident onto the interface between the PV cell and its laminate of glass is absorbed. This allows us to consider only two paths of the incoming light. This allows us to omit surface reflections at the PV-module and to omit the optical paths derived from these reflections.

1. Direct incidence onto the PV cell.
2. Reflection in the retroreflector and then incidence onto the PV-cell.

When the ray intersects with a reflector surface we use a reflection coefficient of 95%, as an average value for the reflection coefficient of alumina throughout the spectral range of c-Si. The solar elevation ( $\psi$ ) is determined from the local latitude ( $\varphi$ ), the declination of the sun ( $\delta$ ) and the azimuth angle ( $\theta$ ) of the sun relative to the local true south:

$$\psi = \sin^{-1} [\sin \varphi \sin \delta + \cos \varphi \cos \delta \cos \theta] \quad (1)$$

The schematic of Fig.1 illustrates the model of the vertical retroreflector, and its orientation relative to earth poles. The model combines the ray tracing with solar irradiation data, obtained by Si-photodetector, which tracks the sun across the sky, and discards the diffuse contribution. We have also tried to include the diffuse solar contribution to the model, simply by adding a fraction of the contribution.

## EXPERIMENTS

The solar irradiance is measured with the tracking solar measurement station illustrated in Fig.2. The tracking device maintains at all time normal incidence of the sun light onto the detector. Further, the solar station provides measurements of the diffuse optical contribution as well as wind speed and temperature. The solar station is mounted above roof height to ensure no shadowing effects from the surroundings.



**FIGURE 2.** (a) The tracking solar setup and (b) the prototyping setup of the bifacial PV cell with its retroreflector are illustrated above.

The prototype is illustrated in Fig.3. The prototype has a cross section which is very similar to the schematics drawn in Fig.1, see Fig.3(a). The height of the PV cell is 1.8 m, while its width and thickness is 0.16 m and 5 mm, respectively. The height of the reflector and the opening in the cabinet is 2 m in order to avoid shadowing effects near the top and bottom of the PV cell. The prototype is mounted at ground level (Fig.3(b)), and therefore, there will be shadowing effects from the surroundings. The data are obtained for direct comparison with our simulations.

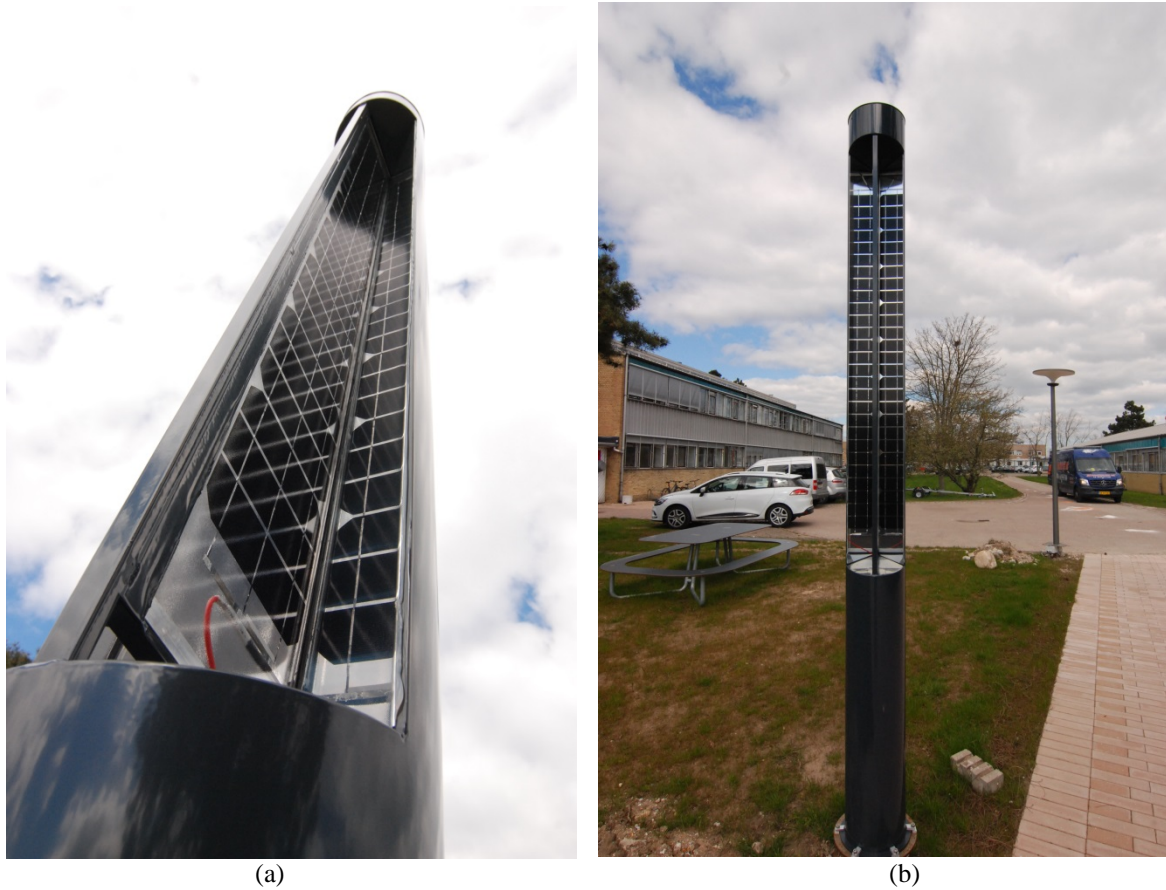


**FIGURE 3.** The prototype, which is mounted on ground level is illustrated above.

The raw data from the systems are sampled with a sample rate of 0.1 S/s. Both, the solar data and the electrical current from the prototype are then low pass filtered with a current averaging algorithm with a flat kernel to an effective sample rate of 0.0042 S/s or approximately 1.0 S/deg. (azimuth angle)

## RESULTS

The latitude is set to  $55.676^\circ$  North, which corresponds to the latitude of Copenhagen. The shortest day (21/12), the longest day (23/6) of the year and the day of data acquisition (10/4) are simulated in our model. Preliminary, we assume that the radiance from the sun is constant during its travel across the sky. The simulations are plotted in Fig.4(a) as the normalized irradiances as a function of azimuthal angle (rad.).

As a reference for the simulations we simulate a bifacial panel facing east-west with the same area as PV cell in the retroreflector a well. Figure 4(b) illustrates the simulations for the bifacial panel.

In Table1 the relative integrated power from the individual curves in Fig.1 and Fig.2 are listed.

Table 1. The normalized power obtained in Fig.4 are integrated through a day and listed for the three dates.

System\Seasons	23 <sup>rd</sup> of June	10 <sup>th</sup> of April	21 <sup>st</sup> of Dec.
Bifacial with retroreflector	0.328	0.348	0.237
Bifacial with no reflector	0.424	0.347	0.102

Clearly, the bifacial PV without a reflector perform best during the summer time when the sun travels through a large azimuth angular interval. However, the bifacial PV cell with the retroreflector perform best during the winter periods where the sun travels through a short angular interval, and with low sun height.

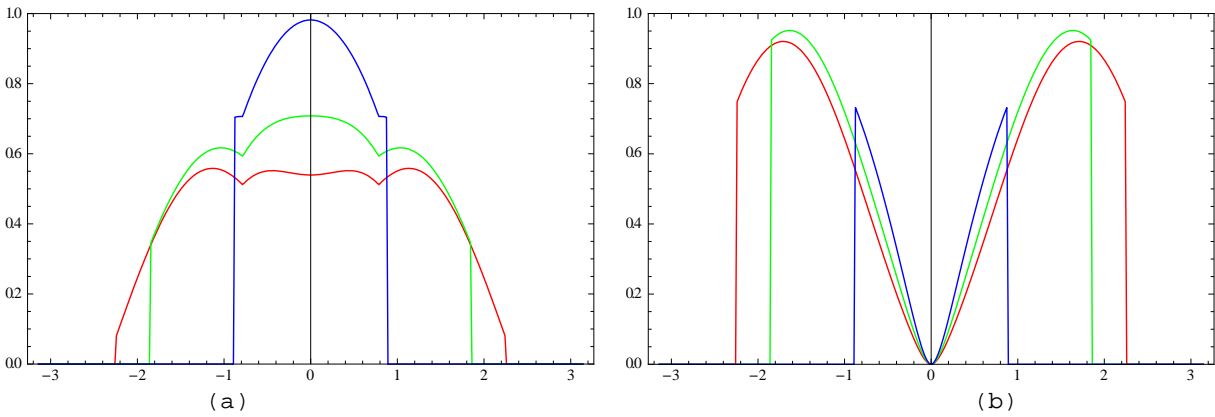


**FIGURE 4.** The simulations of the bifacial PV cell with the retroreflector (a) and the bifacial PV cell without the reflector plotted versus azimuth angle (rad.). Latitude:  $55.676^\circ$  North, Dates: (red) 23/6, (green) 10/4 and (blue) 21/12.

In Fig.5(a) the solar irradiance at normal incidence is plotted as a function of azimuth angle. The data are obtained the 10 of April 2017 near Copenhagen. The sky is not entirely cloud free during the morning. However, during the afternoon we have a reasonably good measurement for comparison with the simulations. Diffuse light is eliminated in this measurement. The diffuse contribution to a detector mounted horizontally is plotted in Fig.5(b).

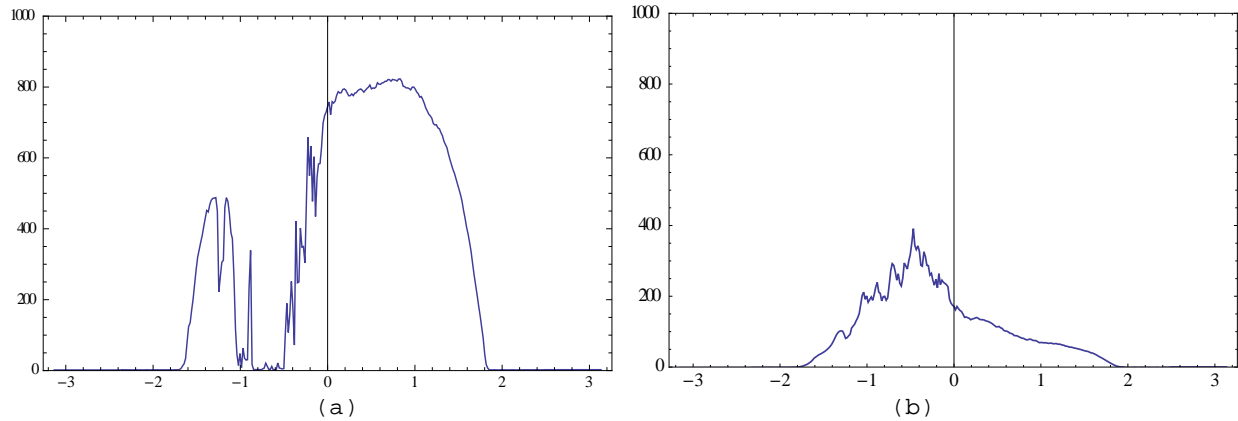


**FIGURE 5.** Solar data obtained near Copenhagen at the 10<sup>th</sup> April 2017 are plotted as a function of azimuth angle (rad.). (a) Illustrates the normal incident light from the sun only, while (b) illustrates the diffuse light contribution to a horizontal surface.

If we multiply the curve in Fig.5(a) with the simulation in Fig.4(a) we find the following simulation for the irradiance incident onto the bifacial PV cell with the retroreflector. The result is plotted it in Fig.6(a). In Fig.6(b) the simulated curve in Fig.4(b) of the reference PV is multiplied with the curve in Fig. 5(b) as well. The integrated power from the two systems for the entire day are 60172 and 49375 respectively. The ratio of these two power values indicating that the bare bifacial PV cell collects only 80% of the power collected by the bifacial PV cell with the reflector.

We have not included the diffuse light in the two curves in Fig.5 because, they are not horizontally mounted as the solar detector, which is responsible for this measurement. Secondly, that the two bifacial PV configurations have different opening angles for diffuse light.

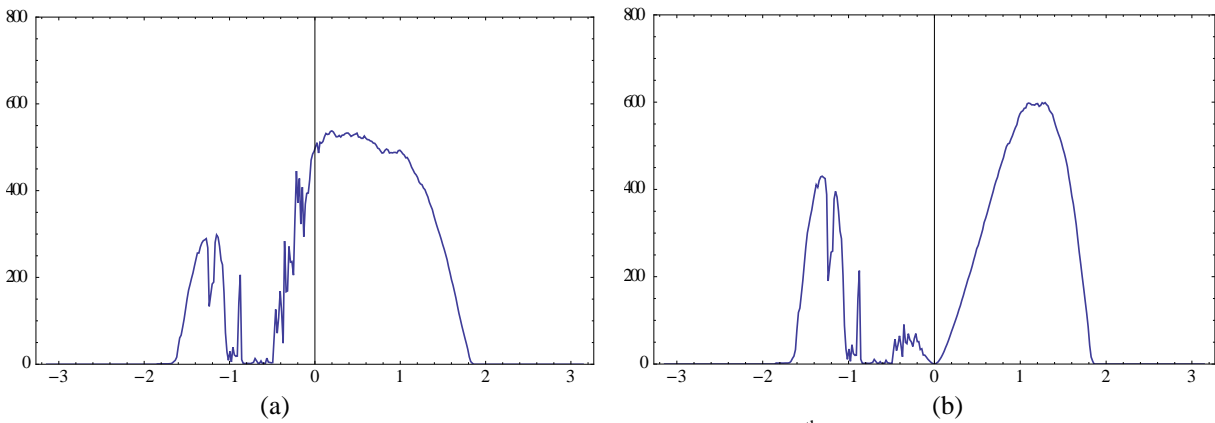


**FIGURE 6.** Simulations of solar power obtained near Copenhagen at the 10<sup>th</sup> April 2017 are plotted as a function of azimuth angle (rad.) for the prototype PV (a) and the reference PV (b).

In Fig.7(a) the measurement from the prototyping bifacial PV cell with retroreflector is plotted. These data are acquired simultaneously with the solar data. In Fig.7(b) the simulated curve including the solar light at normal incidence (Fig.5(b)) has been added half the amount of diffuse light as a simple approach to include the diffuse contribution..

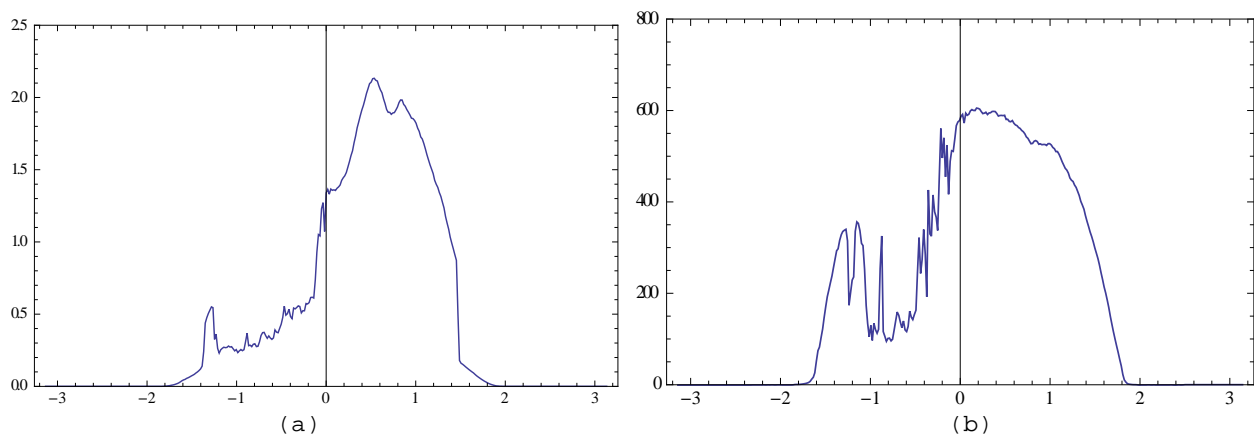


**FIGURE 7.** (a) Solar data obtained near Copenhagen at the 10<sup>th</sup> April 2017 by the prototyping bifacial PV cell with retroreflector is plotted as a function of azimuth angle (rad.) (b) The simulated irradiance including solar data for normal incidence and half the measured amount of diffuse light.

## DISCUSSION

The results in Table1 indicates that by integrating the curves in Fig.4 the prototype and the reference PV provides the same total power for the acquisitions obtained at the 10<sup>th</sup> of April. However, the curves in Fig.6 provide different results for the prototype and the reference PV, which indicates that the reference PV only collects 80% of power collected by the prototype. This is likely to be caused by the attenuation in radiance near sunset, which severely affects the reference PV – compare Fig.4 with Fig.5.

The difference between the measured current produced by the prototype in Fig.7 and the simulated optical irradiance in Fig.6(a) could be caused by issues such as: The semiconductors do not fill out the PV cell entirely as it is assumed for the simulations. Variations in effectivity are expected for the different sub elements in the PV cell. Shadowing effect from the surroundings of the PV cell, like trees or buildings has not been included in the model. Additionally, we do at the moment not have model for including the diffuse light properly in our simulation.

However, by simple adding half the measured diffuse irradiation the observed drop in irradiance (Fig.7(b)) in the interval between -0.8 rad. to -0.6 rad. seems reasonable compare with the measured current Fig.7(a).

## CONCLUSION AND FUTURE WORK

In this work we have completed our simulation by combining the raytracing model with real solar data. Clearly, the simulations conclude that the reflector can have a strong influence on the application of the PV cell. As Table1 illustrates it, the reflector tested with the prototype here has its clear advantages on a Northern latitude compare to the bare bifacial PV cell. Additionally, we have processed our first power measurement from the prototype and compared them with our simulations.

## ACKNOWLEDGMENTS

The project is funded by the Danish Energy Technology Development and Demonstration Programme, project number 64014-0508 “SENSORPOWER – Bifacial PV Energy Reflector Tower”

## REFERENCES

1. G. João, “Testing bifacial PV cells in symmetric and asymmetric concentrating CPC collectors,” *Engineering*, vol. 05, no. 01, pp. 185–190, 2013.
2. A. Moehlecke, F. S. Febras, and I. Zanesco, “Electrical performance analysis of PV modules with bifacial silicon solar cells and white diffuse reflector,” *Sol. Energy*, vol. 96, pp. 253–262, 2013.
3. A. Luque, E. Lorenzo, G. Sala, and S. López-Romero, “Diffusing reflectors for bifacial photovoltaic panels,” *Sol. Cells*, vol. 13, no. 3, pp. 277–292, 1985.
4. R. J. Magasrevy, “Bifacial efficiency at monofacial cost Building Integrated photovoltaic Energy Solutions for the World,” p. 25, 2007.
5. S. Thorsteinsson, M. L. Jakobsen, P. B. Poulsen, P. M. Rødder and K. Rødder, “Vertical reflector for bifacial PV-panels“, part of: IEEE 43rd Photovoltaic Specialist Conference 2016 (ISBN: 9781509027248), pages: 2678-2681, 2016, IEEE.D. L. Davids, “Recovery effects in binary aluminum alloys,” Ph.D. thesis, Harvard University, 1998.
6. M. L. Jakobsen, S. Thorsteinsson, P. B. Poulsen, P. M. Rødder and K. Rødder, “Ray Tracing modelling of a reflector for a vertical bifacial panel“, part of: Proceedings of the 2016 European Photovoltaic Solar Energy Conference and Exhibition 2016, 2016.